

HIGH RESOLUTION X-RAY SPECTROSCOPY OF PRE-MAIN-SEQUENCE STARS: TWA 5 AND PZ TEL

C. Argiroffi¹, J. J. Drake², F. R. Harnden², A. Maggio³, G. Peres¹, S. Sciortino³, B. Stelzer³, and R. Neuhauser⁴

¹Dipartimento di Scienze Fisiche ed Astronomiche, Sezione di Astronomia, Università di Palermo, Piazza del Parlamento 1, 90134 Palermo, Italy

²Smithsonian Astrophysical Observatory, 60 Garden Street, Cambridge, MA 02138

³INAF - Osservatorio Astronomico di Palermo, Piazza del Parlamento 1, 90134 Palermo, Italy

⁴Astrophysikalisches Institut und Universitäts-Sternwarte, Schillergässchen 2-3, D-07745 Jena, Germany

ABSTRACT

We report on the analysis of high resolution X-ray spectra of two pre-main-sequence stars: TWA 5 (observed with *XMM-Newton*) and PZ Telescopii (observed with Chandra/HETGS). TWA 5 is a classical T Tauri star in the TW Hydri association while PZ Tel is a rapidly rotating weak-lined T Tauri star in the β -Pictoris moving group. For both stars we have reconstructed the emission measure distribution and derived the coronal abundances to check for possible patterns of the abundances related to the first ionization potential of the various elements. We have also derived estimates of the plasma density from the analysis of the He-like triplets. We compare the characteristics of our targets with those of other pre-main sequence stars previously analyzed by other authors: TW Hya, HD 98800 and HD 283572. Our findings suggest that X-ray emission from classical T Tauri and weak-lined T Tauri stars is produced in all cases by magnetically-heated coronae, except for TW Hya which has unique plasma temperatures and densities. Moreover we derive that TWA 5 has the same peculiar Ne/Fe abundance ratio as TW Hya.

Key words: Stars: pre-main-sequence – Techniques: spectroscopic – X-rays: stars

The analysis of the X-ray emission allows us to infer the characteristics of the emitting plasma including the thermal structure, the electron densities, and the elemental abundances.

High resolution X-ray spectroscopy studies have been performed for other PMS stars, and in particular for the CTTS TW Hya (Kastner et al. 2002; Stelzer & Schmitt 2004), and for the two WTTs HD 98800 (Kastner et al. 2004) and HD 283572 (Scelsi et al. 2004a). The analysis of TWA 5 and PZ Tel fills the gap between stars characterized by strong H α emission lines, like TW Hya, and active stars near the zero age main sequence (ZAMS) with H α in absorption.

2. TARGET INFORMATION

The principal characteristics of TWA 5 and PZ Tel are reported in Table 1, together with those of the other comparison PMS stars mentioned above. Note that TWA 5

Table 1. Characteristics of the star sample. Negative values of H α equivalent width indicate an emission line.

Name	Mass (M_{\odot})	Spectral Type	Age (Myr)	EW(H α) (Å)	Distance (pc)
TW Hya	~ 0.7	K7	~ 10	-220.00	56
TWA 5	~ 0.5	M1.5	~ 10	-13.64	55
HD 98800	~ 1	K5+K7	~ 10	0.00	47
PZ Tel	~ 1	K0	~ 12	0.63	50
HD 283572	~ 1.6	G2	~ 10	1.12	128

1. INTRODUCTION

The aim of the present work is to investigate the evolution of stellar X-ray emission during pre-main-sequence (PMS) stages. To address this issue we have analyzed the high resolution X-ray spectra of two PMS stars: the classical T Tauri star (CTTS) TWA 5, and the weak-lined T Tauri star (WTTs) PZ Tel (Argiroffi et al. 2004). These two stars allow us to probe different evolutionary phases. Mass accretion is still present in TWA 5 as shown by its asymmetric and broad H α emission (Mohanty et al. 2003). Jayawardhana et al. (1999) suggested a possible infrared excess but this finding has been ruled out by subsequent studies (Metchev et al. 2004; Weinberger et al. 2004), indicating that TWA 5 no longer harbors large amount of dust. The accretion process has just ended in PZ Tel which has a filled in H α line (Soderblom et al. 1998).

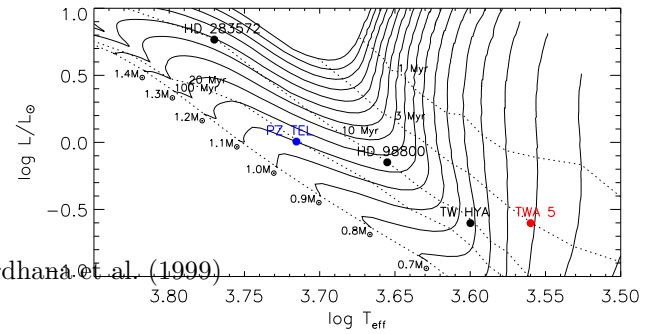


Figure 2. HR diagram with isochrones (dotted lines) and evolutionary tracks (solid lines) from Siess et al. (2000).

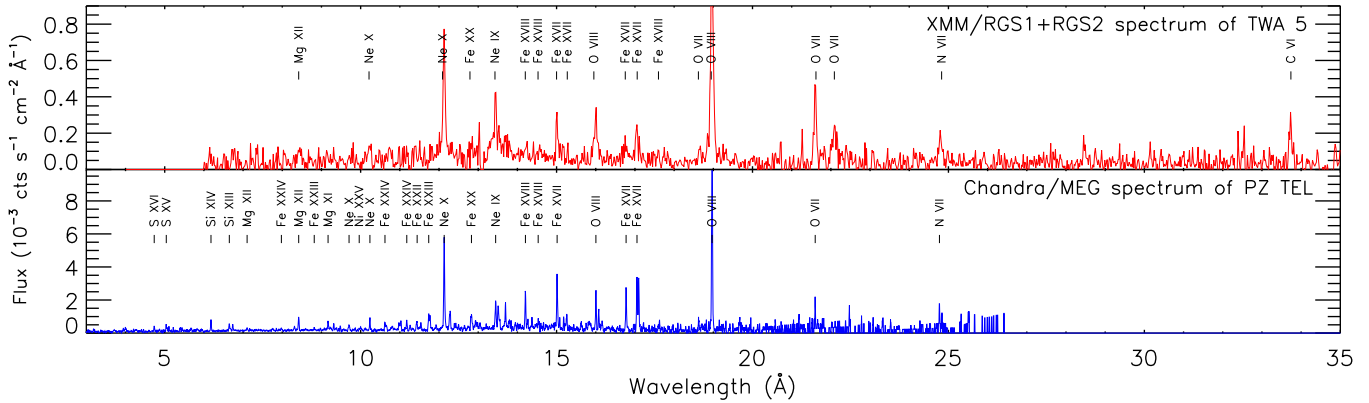


Figure 1. Upper panel: Spectrum of TWA 5 obtained by adding the RGS1 and RGS2 X-ray spectra previously rebinned by a factor 2. Lower panel: Spectrum of PZ Tel obtained by smoothing the Chandra/MEG first order spectra.

is a multiple system: the primary, TWA 5A, is a spectroscopic binary consisting of similar component, while TWA 5B, the secondary, is a M8 brown dwarf. HD 98800 is a quadruple system: it consists of two visible components, each of which is a spectroscopic binary. HD 98800 spectral type in Table 1 refers to the two stars which contribute to the X-ray emission. In Figure 2 we show the location of the stars in our sample on the HR diagram.

3. OBSERVATIONS

TWA 5 was observed with *XMM-Newton* on 2003 January 9, for 29.7 ks. RGS first order spectra were extracted with SAS V5.4.1. As shown by Tsuboi et al. (2003) the X-ray emission of TWA 5 is dominated by the primary component. PZ Tel was observed with *Chandra/HETGS* on 2003 June 7, for 73.9 ks, and we have used CIAO V3.0 to extract first order spectra. In Figure 1 both spectra are shown with labels indicating the strongest emission lines. The observed X-ray luminosities, in the range 6-20 Å, for TWA 5 and PZ Tel are 4.4×10^{29} and 2.2×10^{30} erg s $^{-1}$, respectively.

4. RESULTS

We have reconstructed the plasma emission measure distribution (*EMD*) and derived the coronal abundances for both stars applying the MCMC method (Kashyap & Drake 1998) based on the measured line fluxes. The results obtained are shown in Figures 3 and 4. The continuum adopted for the line fitting agrees with the continuum predicted by the *EMD* and the abundance set for each star. The analysis of PZ Tel has been performed using the CHIANTI database, while for TWA 5 we used the APED database. Note however that these databases provide compatible results with the analysis approach we have followed, as discussed by Scelsi et al. (2004b).

4.1. EMDs

The emission measure distributions that we have derived for both targets (Figure 3) show characteristics similar to those of other active stars, and in particular a peak at $\log T \sim 6.9 \div 7.0$ and steep slopes in the temperature range just preceding the peak. Moreover PZ Tel has a significant amount of plasma at higher temperatures, with another peak at $\log T = 7.3$. The fact that we do not see such hot temperatures in the *EMD* of TWA 5 may be due to a lower average coronal temperature, or to the different diagnostics offered by *XMM-Newton/RGS* in comparison with *Chandra/HETGS*. The analysis of *XMM-Newton/EPIC* data of TWA 5, which will appear in a subsequent paper, will help to answer this question.

4.2. ABUNDANCES

In Figure 4 we show the derived coronal abundances relative to the solar photospheric values (Grevesse & Sauval 1998), this is because photospheric abundances of the relevant stars are not known, and on principle they may differ significantly from solar values. The elements are sorted by increasing first ionization potential (FIP) values. The *EMD* reconstruction based on line fluxes provides relative abundances of elements for which we have measurable lines. We then obtained abundances relative to H by scaling the metallicity so as to match predicted and observed continuum level in line-free spectral region. For both stars we find a pattern with a minimum abundance at intermediate FIP elements, while the elements with higher FIP show higher values of abundance. This behavior is more evident for TWA 5 whose Ne/Fe abundance ratio is ~ 10 times higher than the solar one.

4.3. DENSITIES

We have used the density sensitivity of the intercombination and forbidden lines of He-like ions (Gabriel & Jordan 1969)

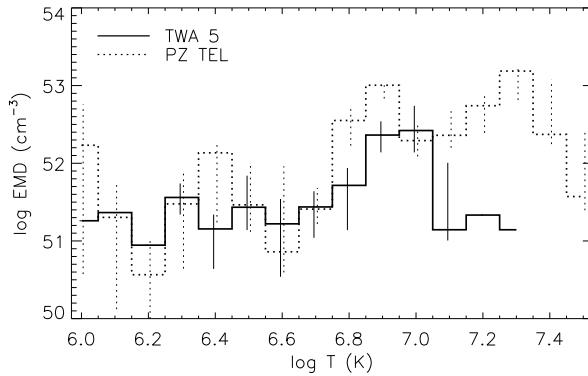


Figure 3. Emission measure distribution of TWA 5 (solid line) and PZ Tel (dotted line).

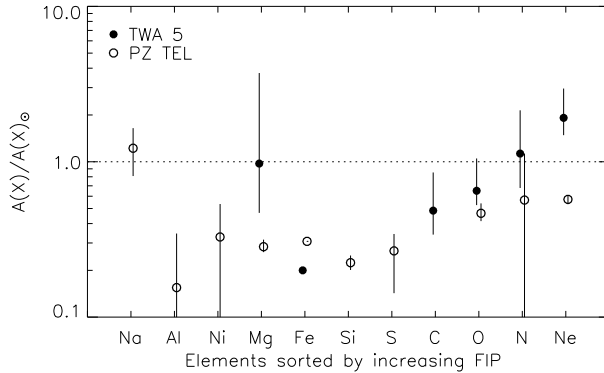


Figure 4. Elemental abundances of TWA 5 (filled symbols) and PZ Tel (open symbols) referred to the solar photospheric values (Grevesse & Sauval 1998).

to investigate the coronal electron densities N_e . In the observed X-ray spectrum of TWA 5 we have analyzed only the O VII triplet, because the Ne IX triplet is blended with Fe XIX lines and the RGS spectral resolution is insufficient to resolve these blends. On the other hand in the observed X-ray spectrum of PZ Tel we have analyzed the Ne IX, Mg XI and Si XIII triplets, while of the O VII triplet only the resonance line has been detected. The O VII He-like triplet for TWA 5 and the Ne IX triplet for PZ Tel are shown in Figures 5 and 6, including observed spectra and best-fit line profiles; the derived N_e values are shown in Table 2. We derive only upper limits for the electron

Table 2. Electron Densities from He-like triplets.

star	ion	$\log T_{\text{max}}$ (K)	f/i	$\log N_e$ (cm $^{-3}$)
TWA 5	O VII	6.3	3.8 ± 2.5	< 11
PZ Tel	Ne IX	6.6	3.0 ± 1.4	< 11.8
PZ Tel	Mg XI	6.8	1.7 ± 0.8	12.6 ± 0.6
PZ Tel	Si XII	7.0	3.5 ± 2.1	< 13.5

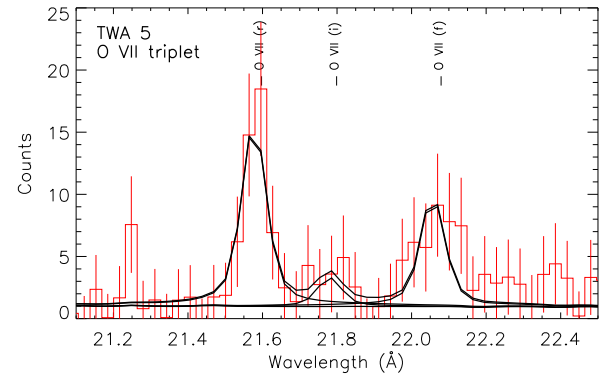


Figure 5. O VII He-like triplet in the TWA 5 spectrum with best fit curves superimposed.

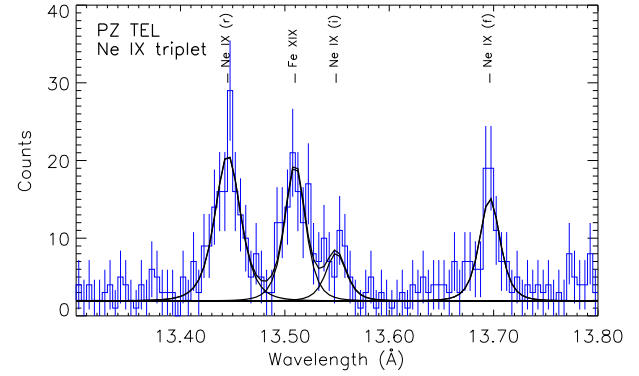


Figure 6. Ne IX He-like triplet in the PZ Tel spectrum with best fit curves superimposed.

densities from the observed f/i ratio for all triplets except the Mg XI for PZ Tel. It is worth noting that these results are different from those of TW Hya where high densities ($N_e \sim 10^{13}$ cm $^{-3}$) have been deduced from the analysis of Ne IX and O VII triplets (Kastner et al. 2002; Stelzer & Schmitt 2004).

5. DISCUSSION

The shape of $EMDs$, the abundance patterns and the electron densities derived from the X-ray spectra of TWA 5 and PZ Tel suggest that the X-ray emission from the PMS stars analyzed is very similar to the coronal emission of more evolved active stars. In the following we compare our results with those of TW Hya, HD 98800 and HD 283572.

5.1. NE/FE ABUNDANCE RATIO

In Figure 7 we compare the Ne/Fe abundance ratios (referred to the solar value) for these five PMS stars sorted by H α equivalent width. Note however that we obtain a similar pattern if our stars are sorted by spectral type.

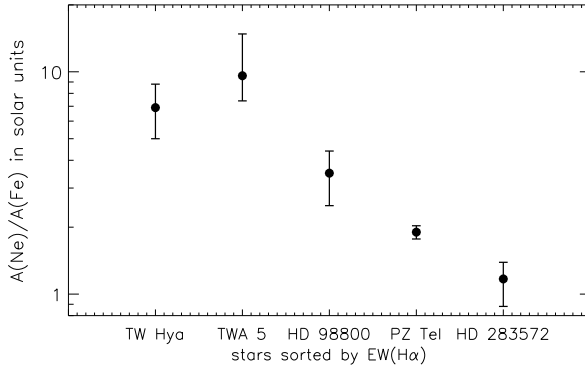


Figure 7. Ne/Fe abundance ratio in solar units (Grevesse & Sauval 1998) for the selected pre-main sequence stars ordered by decreasing $\text{H}\alpha$ emission. We have assumed that the abundance uncertainties of HD 98800 are equal to those of TW Hya, because of the similar S/N ratio of the Chandra spectra of these two stars.

TWA 5 shows the same ratio as TW Hya, while the ratio is significantly lower for the other stars, characterized by no evidence of accretion. This finding suggests that the Ne/Fe abundance ratio may reflect the evolutionary stage of the relevant star, although this interpretation is complicated by the fact that more evolved stars, like the ZAMS K0 dwarf AB Dor, show again very high Ne/Fe values ($\sim 5 \div 10$). While Ne/Fe ratios are also thought to be correlated with stellar magnetic activity, another possibility is that the higher Ne/Fe ratio of TW Hya, TWA 5 and HD 98800, which all belong to the TW Hydreae association, reflects the initial abundances of the cloud from which these stars originated, although this would require rather large variations in local ISM abundances.

5.2. EMD PEAK TEMPERATURE

In Figure 8 we show the *EMD* peak temperatures of the same stars. Note that the HD 98800 value is only indicative because no detailed emission measure analysis has been performed on its data. This plot suggests that the temperature of the emitting plasma rises with the ending of the accretion process, although there are other parameter differences between the selected stars.

6. CONCLUSIONS

In conclusion we have found that Ne/Fe abundance ratio seems to be correlated with evolutionary stages and with spectral type. In particular TWA 5 has the same Ne/Fe abundance ratio as TW Hya. On the other hand, none of the sample stars shows the same densities and plasma temperatures as TW Hya. We can therefore depict two scenarios: in the first case TW Hya may represent CTTSs

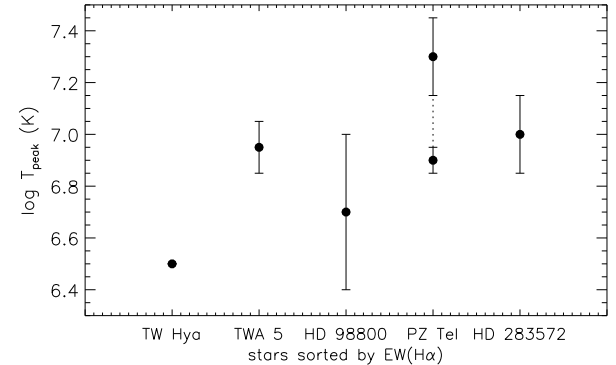


Figure 8. Peak temperature of the *EMD* for the selected pre-main sequence stars ordered by decreasing $\text{H}\alpha$ emission.

with ages ~ 10 Myr, but still characterized by high accretion levels, while the other sample stars represent different evolutionary phases. In the second case TW Hya, and/or its environment, may be quite different from the other CTTSs, and therefore it is not straightforward to reconcile its characteristics with those of the other PMS stars.

ACKNOWLEDGEMENTS

CA, AM, GP, and SS acknowledge partial support for this work by ASI and MIUR. CA acknowledges ESA for travel support.

REFERENCES

- Argiroffi C., Drake J. J., Maggio A., Peres G., Sciortino S., Harnden F. R., 2004, ApJ, 609, 925
- Gabriel A. H., Jordan C. 1969, MNRAS, 145, 241
- Grevesse, N., Sauval, A. J. 1998, Space Science Reviews, 85, 161
- Jayawardhana R., Hartmann L., Fazio G., Fisher R. S., Telesco C. M., Piña R. K., 1999, ApJL, 521, L129
- Kashyap V., Drake J. J., 1998, ApJ, 503, 450
- Kastner J. H., Huenemoerder D. P., Schulz N. S., Canizares C. R., Li J., Weintraub D. A., 2004, ApJL, 605, L49
- Kastner J. H., Huenemoerder D. P., Schulz N. S., Canizares C. R., Weintraub D. A., 2002, ApJ, 567, 434
- Metchev S. A., Hillenbrand L. A., Meyer M. R., 2004, ApJ, 600, 435
- Mohanty S., Jayawardhana R., Barrado y Navascués D., 2003, ApJL, 593, L109
- Scelsi L., Maggio A., Peres G., 2004a, submitted
- Scelsi L., Maggio A., Peres G., Gondoin P., 2004b, A&A, 413, 643
- Siess L., Dufour E., Forestini M., 2000, A&A, 358, 593
- Soderblom D. R., King J. R., & Henry T. J., 1998, AJ, 116, 396
- Stelzer B., Schmitt J. H. M. M., 2004, A&A, 418, 687
- Tsuboi Y., Maeda Y., Feigelson E. D., Garmire G. P., Chartas G., Mori K., Pravdo S. H., 2003, ApJL, 587, L51

Weinberger A. J., Becklin E. E., Zuckerman B., Song I., 2004,
AJ, 127, 2246